

(4)

# A TRIDENT SCHOLAR PROJECT REPORT

AD-A216 324

NO. 163

THE BEHAVIOR OF A COMPOSITE MATERIAL IN COMPRESSION



UNITED STATES NAVAL ACADEMY  
ANNAPOLIS, MARYLAND

This document has been approved for public release and sale; its distribution is unlimited.

DTIC  
ELECTED  
JAN 02 1990  
S B D

96 1 00 064

## UNCLASSIFIED

SECURITY CLASSIFICATION OF THIS PAGE (When Data Entered)

REPORT DOCUMENTATION PAGE		READ INSTRUCTIONS BEFORE COMPLETING FORM
1. REPORT NUMBER U.S.N.A. - TSPR; no. 163 (1989)	2. GOVT ACCESSION NO.	3. RECIPIENT'S CATALOG NUMBER
4. TITLE (and Subtitle) THE BEHAVIOR OF A COMPOSITE MATERIAL IN COMPRESSION.		5. TYPE OF REPORT & PERIOD COVERED Final 1988/89
		6. PERFORMING ORG. REPORT NUMBER
7. AUTHOR(s) Matthew L. Welborn		8. CONTRACT OR GRANT NUMBER(s)
9. PERFORMING ORGANIZATION NAME AND ADDRESS United States Naval Academy, Annapolis.		10. PROGRAM ELEMENT, PROJECT, TASK AREA & WORK UNIT NUMBERS
11. CONTROLLING OFFICE NAME AND ADDRESS United States Naval Academy, Annapolis.		12. REPORT DATE 14 July 1989
		13. NUMBER OF PAGES
14. MONITORING AGENCY NAME & ADDRESS (if different from Controlling Office)		15. SECURITY CLASS. (of this report)
		15a. DECLASSIFICATION/DOWNGRADING SCHEDULE
16. DISTRIBUTION STATEMENT (of this Report)  This document has been approved for public release; its distribution is UNLIMITED.		
17. DISTRIBUTION STATEMENT (of the abstract entered in Block 20, if different from Report)		
18. SUPPLEMENTARY NOTES Accepted by the U.S. Trident Scholar Committee.		
19. KEY WORDS (Continue on reverse side if necessary and identify by block number) Fibrous composites Composite material Fracture Fatigue		
20. ABSTRACT (Continue on reverse side if necessary and identify by block number)  In the study of unidirectional composite materials, the fiber-matrix support mechanism is well understood for the case of a tensile load. Under a purely compressive load, however, the behavior of the fibers in the composite is much less well understood. At present, a widely discussed model of the behavior of the composite is that, under an axial compressive load, the fibers will deform slightly into the shape of a sine wave of very small (OVER)		

*SECRET*

UNCLASSIFIED

SECURITY CLASSIFICATION OF THIS PAGE (When Data Entered)

amplitude. This model has been termed "microbuckling". The objective of the project was to observe and to quantify this phenomenon of microbuckling in a graphite-epoxy composite. It was found that in properly prepared specimens the microbuckling and its associated wavelength were directly observable. From measurements made of the strains in the composite specimen using both surface-mounted resistive strain guages and electrical resistance of the graphite fibers, the amplitude of the observed microbuckling was calculated. As a significant consequence of this determination of the amplitude and wavelength of the microbuckling, it was learned that the fibers in a composite structure under a compressive load are actually subject to two types of strain. The first is the compressive strain that is read by the usual, resistive strain guage and the other, a strain at the spatial frequency of the microbuckling, is alternately tension and compression. This latter strain varies too sharply with distance for all but the smallest strain guages to read, and, in fact, was not sensed directly in the present work. However, it appears that this varying strain is the major component of the compressive strain, and that it was responsible for the failures of the test specimens. In brief, the results of the project are the visual observation of microbuckling, a calculation of its amplitude, and a determination that the associated strain is likely to be an important cause of failure in composite structures in compression.

Accession For	
NTIS GRA&I	<input checked="" type="checkbox"/>
DTIC TAB	<input type="checkbox"/>
Unannounced	<input type="checkbox"/>
Justification	
By _____	
Distribution/ _____	
Availability Codes	
Avail and/or Special	
DIST	R-1

S/N 0102-LF-014-6601

UNCLASSIFIED

SECURITY CLASSIFICATION OF THIS PAGE (When Data Entered)

U.S.N.A. - Trident Scholar project report; no. 163 (1989)

**THE BEHAVIOR OF A COMPOSITE MATERIAL IN COMPRESSION**

A Trident Scholar Project Report

by

Midshipman First Class Matthew Lee Welborn, Class of 1989

U. S. Naval Academy

Annapolis, Maryland

Ole M. Rask

Associate Prof. O. N. Rask  
Weapons & Systems Eng. Dept.

Accepted for Trident Scholar Committee

Dennis F. Hasson

Chairperson

7/14/89

Date

USNA-1531-2

**THE BEHAVIOR OF A COMPOSITE MATERIAL IN COMPRESSION**

Matthew L. Welborn

United States Naval Academy

**ABSTRACT**

In the study of unidirectional composite materials, the fiber-matrix support mechanism is well understood for the case of a tensile load. Under a purely compressive load, however, the behavior of the fibers in the composite is much less well understood. At present, a widely discussed model of the behavior of the composite is that, under an axial compressive load, the fibers will deform slightly into the shape of a sine wave of very small

amplitude. This model has been termed "microbuckling". The objective of this project was to observe and to quantify this phenomenon of microbuckling in a graphite-epoxy composite. It was found that in properly prepared specimens the microbuckling and its associated wavelength were directly observable. From measurements made of the strains in the composite specimen using both surface-mounted resistive strain gauges and electrical resistance of the graphite fibers, the amplitude of the observed microbuckling was calculated. As a significant consequence of this determination of the amplitude and wavelength of the microbuckling, it was learned that the fibers in a composite structure under a compressive load are actually subject to two types of strain. The first is the compressive strain that is read by the usual, resistive strain gauge and the other, a strain at the spatial frequency of the microbuckling, is alternately tension and compression. This latter strain varies too sharply with distance for all but the smallest strain gauges to read, and, in fact, was not sensed directly in the present work. However, it appears that this varying strain is the major component of the compressive strain, and that it was responsible for the failures of the test specimens. In brief, the results of the project are the visual observation of microbuckling, a calculation of its amplitude, and a determination that the

associated strain is likely to be an important cause of failure in composite structures in compression.

## TABLE OF CONTENTS

I.	Introduction: Composite Materials .....	5
II.	The Fiber-Matrix Mechanism .....	6
III.	Electrical Resistance as an Indicator of Strain .....	9
IV.	Test Sample Construction .....	11
V.	Test Method .....	13
VI.	Data Collection .....	15
A.	Distance Measurements .....	15
B.	Strain Measurements .....	15
C.	Resistance Measurements .....	15
D.	Visual Measurements .....	16
E.	Failure of Specimens .....	16
VII.	Experimental Results .....	17
VIII.	Conclusions .....	19
IX.	Future Work .....	20
X.	References .....	22
XI.	Illustrations .....	24
XII.	Appendices .....	32

## INTRODUCTION: COMPOSITE MATERIALS

The quantitative characterization of materials has been important for as long as man has been building structures. In the past twenty years or so, there have been rapid developments of new types of materials known as composite materials. As the name suggests, a composite material is one that is made up of two or more different phases, primarily to take advantage of the desirable properties of each of the different phases. One of the most useful forms of composite material is one in which a fibrous phase is imbedded in a supporting matrix. Of these fiber-matrix composites, one of the most widely used is made of graphite fibers in an epoxy matrix.

It was known as early as the 1960's that carbon rich materials, such as rayon fibers or pitch, could, with the aid of heat in an inert atmosphere, be converted into graphite fibers. These graphite fibers can be produced in any length desired, and are about seven millionths of a meter in diameter. It is a property of these, and indeed many fibers, that their strength and stiffness per unit weight vastly exceed these properties for the same material in bulk form. This physical fact is due to flaws and dislocations which are present in the bulk form, but

not in fiber form.

Because of the one-dimensional nature of these fibers, it is possible to embed the fibers in a supporting matrix in such a way that the fibers are aligned only in certain specific directions, thus creating a structure in which the great axial strength and stiffness of the fibers support external loads which lie along these same directions. Using this technique, strength and stiffness can be avoided in directions of little or no load, resulting, typically, in a large savings in weight and size. This is of great importance in applications such as aircraft design, where any savings in structural weight can justify the higher costs associated with composite materials.

#### THE FIBER-MATRIX MECHANISM

The actual mechanism through which a fiber-matrix composite supports an external load is highly dependent upon the type of loading that is present. For a load of pure tension, the interaction of the fibers and the matrix is very straightforward. When a tensile load is applied to a composite structure such as that in Figure 1, the great axial strength and stiffness of the internal fibers allow the fibers to support almost all of the load. The fibers remain straight because they are in tension, and the

surrounding matrix serves to support and protect the fibers while carrying very little of the external load.

If the same structure were to be subjected to a compressive load as shown in Figure 2-a, however, the interaction between the fibers and the matrix is much more complex. In this case, the matrix plays a crucial role in supporting the external load. Although the great axial strength and stiffness of the fibers may still be sufficient to support the axial load, the surrounding matrix must hold the fibers straight or the structure will be unable to resist the load and will collapse.

This complex interaction between the fibers and the supporting matrix of a composite structure is one of the least understood aspects of composite material technology. Also, this very interaction makes it difficult to directly observe the internal behavior of the composite under compression. Opening the structure to observe the fibers under load would necessitate the removal of the supporting matrix, which would defeat the load-bearing mechanism.

One of the most widely discussed theories of the fiber-matrix mechanism under compression postulates a phenomenon known as "microbuckling". When a composite structure is under axial compression, the fibers do still support the load, but because the matrix is usually much less stiff than the fibers one can readily imagine that

distortion of the fibers as sketched in Figure 2-b occurs. We model the periodic wave form in Figure 2-b as a sine wave. It was the goal of this work to look for and study this microbuckling phenomenon, and to understand its consequences if found.

## ELECTRICAL RESISTANCE AS AN INDICATOR OF STRAIN

The graphite-epoxy composite which has been the subject of research in this project is unusual among composites in that it has some very interesting electrical properties. The graphite fibers which provide the great strength and stiffness of this composite have a relatively low electrical resistivity. The epoxy used for the matrix, however, has a high resistance to electrical current and is, in effect, an insulator. Thus, if a measurement is made of the electrical resistance through a hardened composite, it is reasonable to conclude that the current is actually flowing through the fibers and not through the surrounding matrix.

In a Trident project completed in 1987, Midshipman First Class David A. Robinson carried out a study of failure in graphite-epoxy composites. The primary conclusion of his report was that in a composite specimen such as that shown in Figure 3, the electrical resistance measured end-to-end through the layer of graphite fibers could actually be used as a measure of internal damage to the graphite fibers. He found that when the specimen began to fail, some of the internal fibers would break and this would cause an increase in the measured resistance. This

phenomenon is represented in Figure 4.

A secondary finding in the report was that before these fibers began to break, there would be smaller, but still measurable, changes in the electrical resistance with strain. When such a specimen was put in tension, the resistance would increase slightly; when the same specimen was put in compression, the resistance would decrease slightly. His conclusion was that these changes in electrical resistance, measured prior to any damage to the fiber, were actually caused by the changes in the strain of the fiber. If this were true, then the measurement of resistance through the internal fibers could be thought of as an indicator of the state of strain of the fibers.

This conclusion is easier to understand in terms of the individual fibers. If a single fiber were placed in tension, it should become longer and thinner, as in Figures 5-a and 5-b. This tensile strain should be accompanied by an increase in electrical resistance. On the other hand, if the fiber were placed in compression, it would be expected to become shorter and thicker. This compressive strain should be accompanied by a corresponding decrease in electrical resistance. This idea is illustrated in Figure 5-c.

Because of the difficulty involved in observing the interior of a composite specimen in a state of stress, the

use of electrical resistance measurements to reveal the strain in the graphite could be very important. Although the actual variation of the electrical resistivity of graphite fibers under strain is not known, it will be assumed for the purpose of this work that this property is a constant of the material and is not in any way dependent on the shape into which the fibers are strained. It was determined in earlier work that over the normal range of room temperature, electrical resistivity does not vary with temperature.

#### TEST SAMPLE CONSTRUCTION

The test samples are very similar to those used by Midshipman Robinson that were shown in Figures 3 and 4. In addition to the electrical resistance measurements used in the earlier work, it was decided to also employ conventional, surface-mounted strain gauges.

The graphite used in the specimens was produced by the Orcon Corporation and is termed Orcoweb G-900. Before the graphite layers could be laminated into a composite specimen, there had to be a provision for electrical connection to the graphite fibers themselves. To do this, each end of each of the layers of graphite fibers was saturated with conductive silver paint. To this paint, metal tabs cut from 0.001 inch brass shim stock were

attached. These tabs made it very simple to measure the electrical resistance through each layer of graphite once the insulating epoxy had been added and was hardened.

The actual structure of the laminated composite was dictated by several important considerations. There would be two separate layers of graphite fibers in the specimen, and these two layers would be separated by four layers of glass fibers. The glass used was eight ounce, bidirectional E glass, a common material in fiberglass aircraft construction. The inner glass layers served to electrically isolate the two layers of graphite fibers. This is important because the resistance measured through each of the layers of graphite needed to be distinct. Also, the layers of glass in the middle of the specimen served to provide physical separation between the two layers of graphite which, when the sample was deflected, resulted in a compressive strain on the concave surface and a tensile strain on the convex surface.

To make the final composite specimen, the materials are united in what is termed a hand lay-up process. The epoxy used as the matrix was called System West 105, and was manufactured by the Gougeon Corporation. The process begins when a graphite layer wetted with epoxy is put down on a flat surface lightly coated with mold-release. Then, one at a time, glass layers and epoxy are added and,

finally, the second graphite layer is put on the top. In this work, the surface on which the specimen was laid-up was an optical flat. When used as a base for the lamination process, it provided a surface on the finished composite that was as smooth as a mirror. The idea behind this was an attempt to make any microbuckling obvious on the surface of the specimen.

The last step in the construction of each specimen was the application of a Micro-Measurements resistive strain gauge on each side of the specimen. The actual gauges used were type EA-06-250-FB-350. Since the strain of interest was along the fibers, the gauges were aligned lengthwise. They were used in the quarter-bridge configuration, and each gauge had an active length of five-sixteenths of an inch.

#### TEST METHOD

In order to study the behavior of the composite under compressive loads along the axis of the fibers, it was necessary to find a method to place the specimen under stress which was both non-destructive and would provide data which were relatively easy to interpret. It is easy to imagine placing a specimen under a compressive load by simply applying a compressive force to each end of the

specimen along its axis. This method would provide strains that could easily be interpreted, but it is unacceptable for several reasons. First, the electrical contact between each metal tab and the fibers is very delicate; placing this portion of the specimen under stress would damage the connections and cause erroneous resistance readings. Also, if the beam were simply compressed along its axis, it would Euler buckle away from the line of the force and structures which have Euler buckled can, in many applications, be said to have failed.

The method which was chosen to load the composite is known as a four-point bend, and is shown in Figure 7-a. In this method, the specimen is mounted between four bending points in a Material Testing System (MTS). The MTS allows the amount of the bend to be very precisely controlled, as in Figure 7-b. This precise measurement of the deflection of the beam, in addition to an understanding of the structure of the beam, makes it possible to calculate the exact stress at any point along the beam.

The actual testing of each of the specimens would involve mounting the specimen between the bending points and decreasing the distance between the upper and lower bending mounts in small steps. In this way, the specimen was placed under an increasing bending moment and

measurements of mechanical strain and electrical resistance were taken at each small increment in the bending process.

#### DATA COLLECTION

##### DISTANCE MEASUREMENTS

As is shown in Figure 7-b, the displacement of the bottom bending fixture from its original position is labeled D<sub>1</sub>, and this was used to index the data. All measurements were taken as D<sub>1</sub> was incremented 0.010 inches at a time. The displacement was actually measured two ways; it was measured both on the MTS machine, and with a separate mechanical dial indicator gauge. The displacement of the center of the beam from its original position, D<sub>2</sub>, was also measured with a dial gauge, and used in the analysis of the geometry of the beam.

##### STRAIN MEASUREMENTS

The strain gauges were placed in the center of the specimen as shown in Figure 7-c. One of the gauges measured the tension in the bottom surface, and the other measured the compression in the top surface.

##### RESISTANCE MEASUREMENTS

The electrical resistances of the graphite surfaces

were measured using the Wayne-Kerr resistance meter which employs a four-contact system. Typical resistance values were in the vicinity of  $0.7\Omega$  and were measured to an accuracy of  $+/-0.0003\Omega$ .

#### VISUAL MEASUREMENTS

The specimen was deflected with the mirror-smooth surface in compression. It remained smooth as viewed in reflected light until the strain gauge readings were in the vicinity of 0.1% strain. At this point, obvious periodic ripples appeared rather abruptly in the surface of the specimen. Their mechanical wavelength was measured to be  $0.050 +/- 0.005$  inches. The ripples were quite uniform and extended over the entire length of the compressed surface between the two upper bending points. This periodic rippling is represented in Figure 8.

#### FAILURE OF SPECIMENS

At specimen deflections just slightly greater than those at which the microbuckling first became visible, the specimen would typically fail. This failure would take the form of a single line across the compressive surface of the specimen, along the wavefront of the microbuckling. At failure, the compressive strain gauges would typically indicate only about one to two tenths of a percent strain.

A further indication of the failure would be relatively large otherwise unexplained increase in the electrical resistance measured through the compressed graphite fibers once they were unloaded. This increase is surely similar to that observed by Midshipman Robinson in his study of composite failure.

#### EXPERIMENTAL RESULTS

The objective of the research carried out for this project was to confirm and study the microbuckling hypothesis. The first direct observation of the microbuckling occurred when the mirror-smooth surface of the composite specimens was compressed and the deformation of the surface into a periodic wave was noted. At the same time, it was possible to estimate the wavelength of this microbuckling at about 0.05 inches. This wavelength was fairly consistent for all of the specimens in which the buckling was observed.

The interpretation of the measurements obtained by the strain gauges is also consistent with the model of the microbuckling of the layer in compression. For this interpretation, the published ratio of the graphite modulus in compression to that in tension was used to calculate the ratio of expected strains on the compressive surface to

those on the surface in tension. We found this ratio to be considerably greater than the observed ratio of strains as measured by the strain gauges. If two points were marked on the surface to be compressed, they would move much closer together in compression than is indicated by the contact strain gauges. We attribute this additional closing of these two hypothetical points to microbuckling.

Mathematically, we can relate the length along a sine wave and its wavelength to its amplitude. In this way, the difference between the predicted compressive strain and the measured compressive strain can be used to get the otherwise unavailable amplitude of the microbuckling. A sample calculation of this amplitude for a typical specimen can be found in Appendix F.

The final confirmation of microbuckling is obtained from the fact that the specimens always failed in compression at a measured strain in the range of one to two tenths of a percent. This is far below the limits published for graphite-epoxy composites. However, when the amplitude of the microbuckling is used to calculate additional alternating strains which had been averaged out by the contact strain gauges, it was found that the specimens at failure were experiencing strain of over two percent. This is more than sufficient strain to cause failure.

The interpretation of the electrical resistance readings is very similar to the interpretation of the mechanical strain readings, although less sensitive. Assuming that the changes in resistance are proportional to strain, then the ratio of the resistance change in compression to that in tension should be the same as the predicted strain ratios, if not higher. As was true with the ratio of measured strains, however, the actual ratio of resistance changes was much lower than predicted and is accounted for in this work by the assumption of microbuckling of the graphite layer. In this way, both the strain measurements and the electrical measurements support the microbuckling model.

#### CONCLUSIONS

Several conclusions have been drawn concerning the nature of the microbuckling phenomenon. First of all, the microbuckling effect can be made visible on the surface of a graphite-epoxy composite specimen. Also, from this visible microbuckling, a very good estimate of the wavelength can be obtained, and for this particular combination of graphite fibers and epoxy matrix, the wavelength was observed to be about fifty one-thousanths of an inch.

The use of surface-mounted resistive strain gauges to

measure the average strain over the surface was helpful in not only confirming the presence of microbuckling, but also in obtaining its actual amplitude. The measurements of electrical resistance were also of help in confirming the presence of microbuckling, but were of limited use in quantitative analysis of the microbuckling.

One important practical results of the work is the understanding of the relationship between a strain gauge and the surface upon which it is mounted. Our gauges were approximately 0.300 inches long, and the wavelength of the microbuckling was only 0.050 inches. This means that the gauge would actually cover six or seven wavelengths of the buckling. The strain gauge gave only the average strain, not the peak strain. It would have been necessary to use strain gauges only 0.010 inches long to detect the actual strains. If it is not practical to apply such tiny strain gauges on real structures, then it might be possible to form on the surface of the critical regions of such real structures a flat surface on which microbuckling would be visually evident.

#### FUTURE WORK

Future work of importance could be done to predict the actual microbuckling wavelength for different composites.

Also, it might be possible to develop a technique using infra-red or optical means to measure the amplitude of the observed buckling.

## REFERENCES

1. Gause, L. W. and Alper, J. M., "Braided to Net Section Graphite/Epoxy Composite Shapes," Journal of Composites Technology & Research, Vol. 10, No. 2, Summer 1988, pp. 33-46.
2. Greszczuk, L. B., "Microbuckling of Unidirectional Composites," AFML Technical Report AFML-TR-71-231, Air Force Materials Laboratory, Wright-Patterson Air Force Base, Ohio, 1972.
3. Hull, Derek, An Introduction to Composite Materials, Cambridge: Cambridge University Press, 1981.
4. Lanir, Y. and Fung, Y. C. B., "Fiber Composite Columns Under Compression," Journal of Composite Materials, Vol. 6, July 1972, p. 387.
5. Lifshitz, J. M., "Compressive Fatigue and Static Properties of a Unidirectional Graphite/Epoxy Composite," Journal of Composites Technology & Research, Vol. 10, No. 3, Fall 1988, pp. 100-106.

6. Mallick, P. K., Fiber-Reinforced Composites: Materials, Manufacturing, and Design, New York: Marcell Dekker, INC., 1988.
7. McCollough, R. L., Concepts of Fiber-Resin Composites, New York: Marcell Dekker, INC., 1971.
8. Rask, Olaf N. and Robinson, David A., "Graphite as an Imbedded Strain Gauge Material," SAMPE Journal, January/February 1988, pp. 33-46.
9. Robinson, David A., Failure Modes in Composite Materials, USNA Trident Project Report, 1987.



FIGURE 1: COMPOSITE IN TENSION



FIGURE 2-a: COMPOSITE IN COMPRESSION

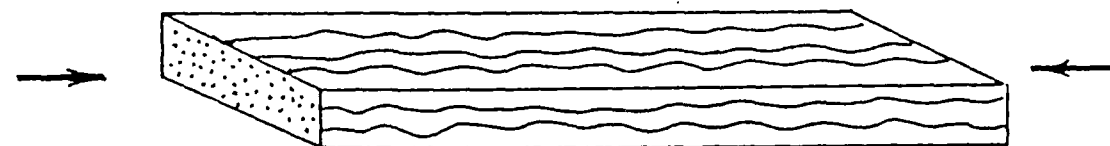


FIGURE 2-b: COMPOSITE IN COMPRESSION -  
MICROBUCKLING PRESENT

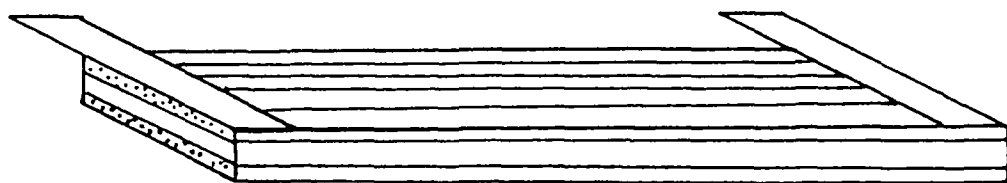


FIGURE 3: COMPOSITE BEAM WITH CONTACTS TO MEASURE ELECTRICAL RESISTANCE

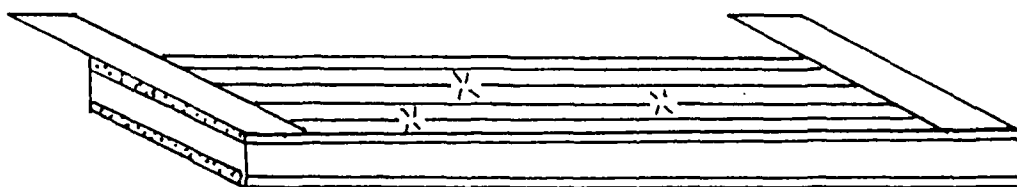


FIGURE 4: BROKEN GRAPHITE INDICATED BY INCREASED RESISTANCE



FIGURE 5-a: GRAPHITE FIBER - NO STRAIN

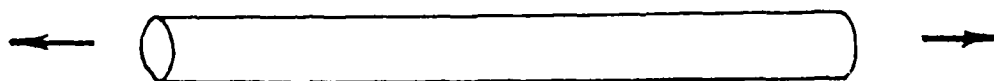


FIGURE 5-b: GRAPHITE FIBER - TENSILE STRAIN

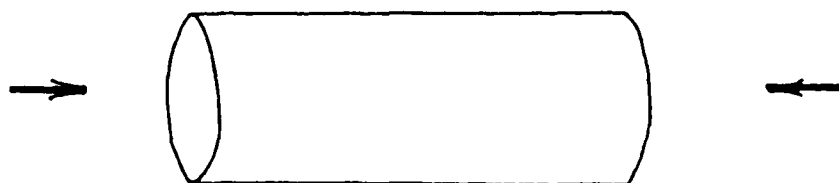


FIGURE 5-c: GRAPHITE FIBER - COMPRESSIVE STRAIN

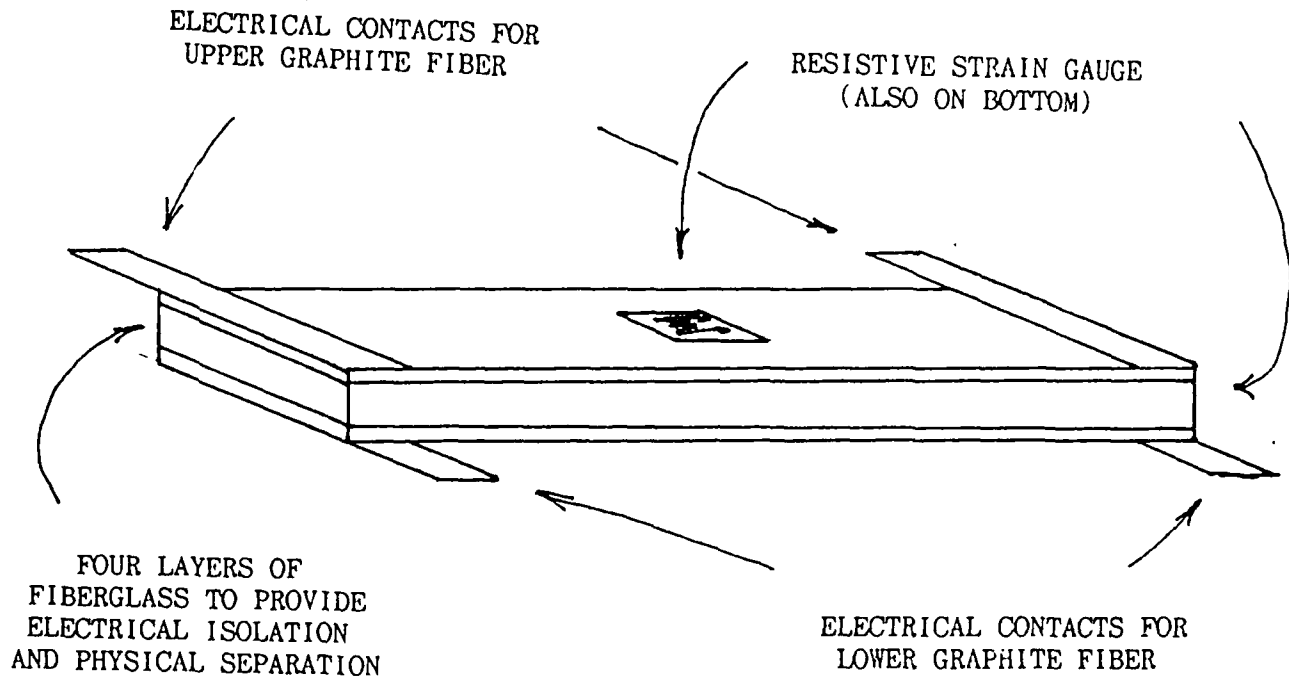


FIGURE 6: COMPLETE COMPOSITE SPECIMEN

FIGURE 7-a: SPECIMEN MOUNTED IN FOUR-POINT BEND APPARATUS

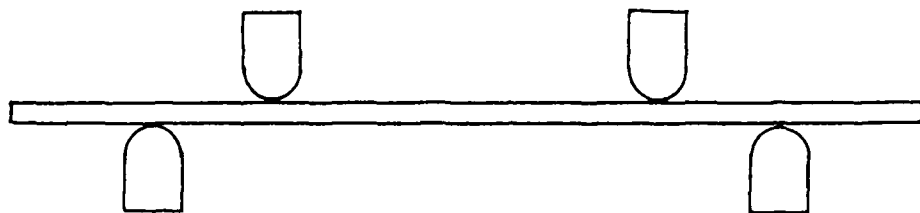


FIGURE 7-b: SPECIMEN BEING DEFLECTED

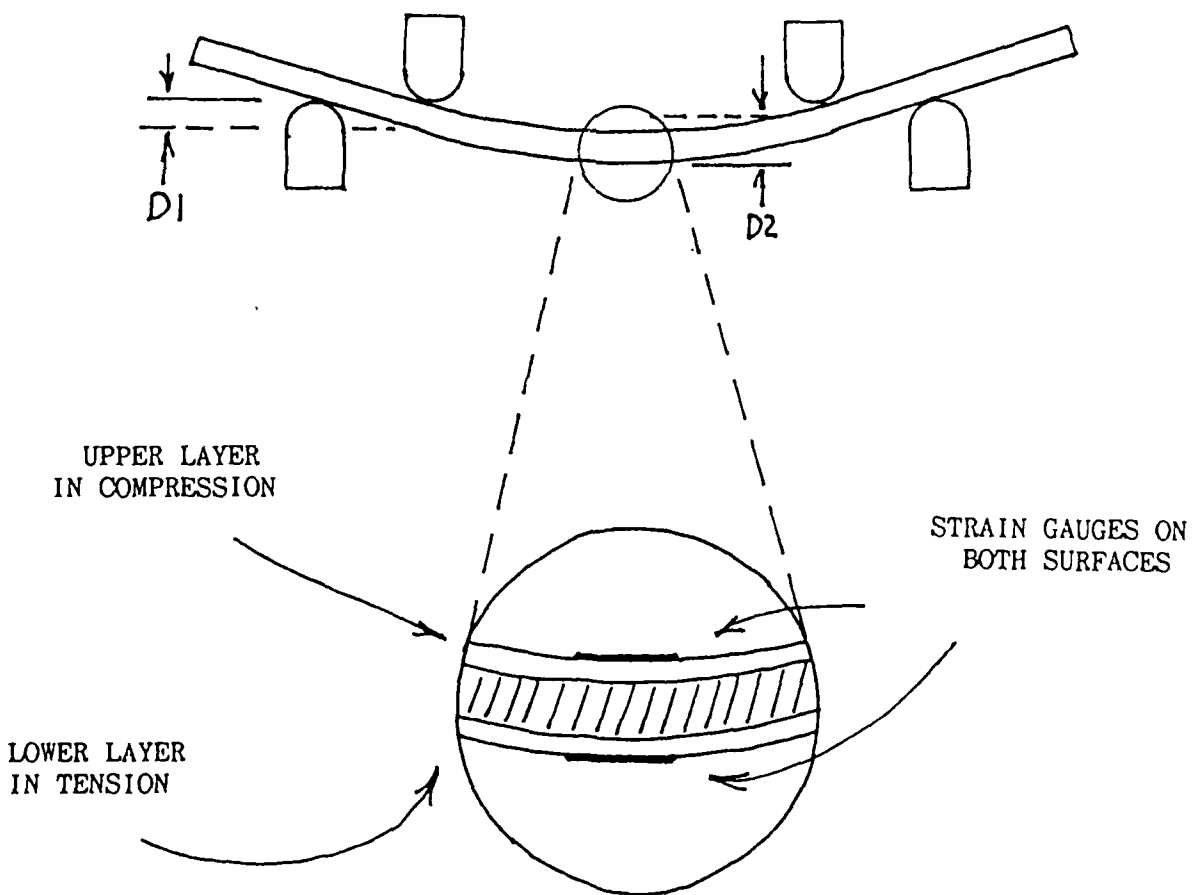


FIGURE 7-c: ENLARGED VIEW OF SPECIMEN

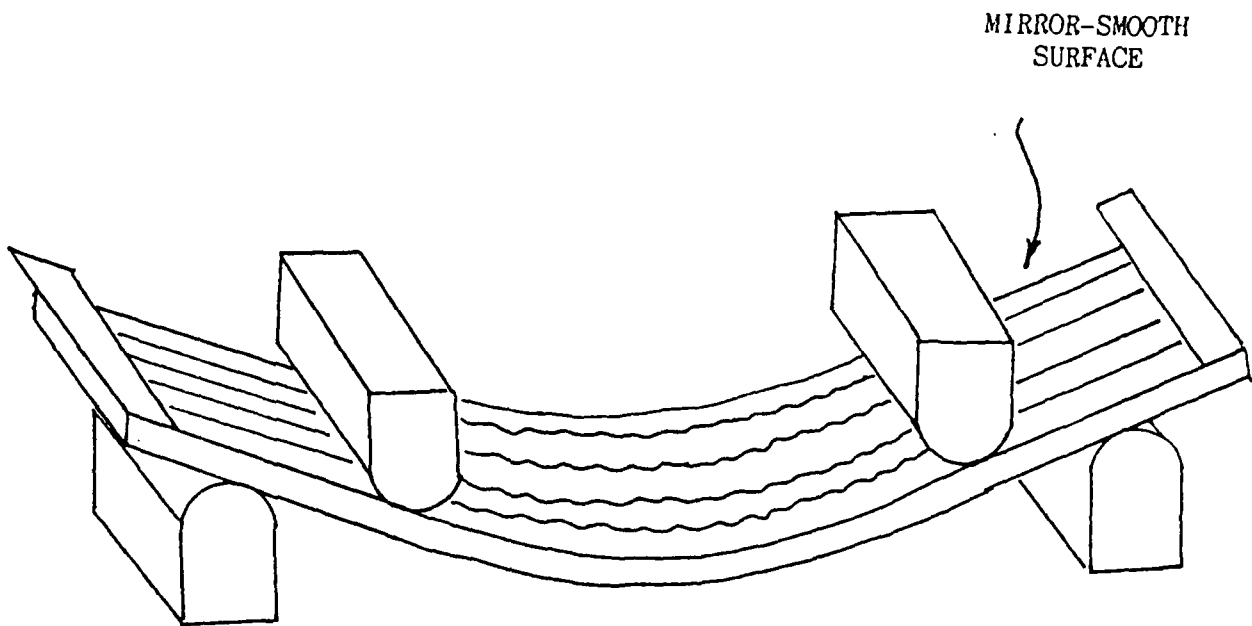


FIGURE 8: DIRECT OBSERVATION OF MICROBUCKLING

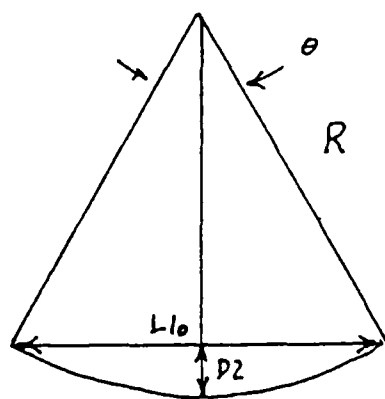


FIGURE A-1

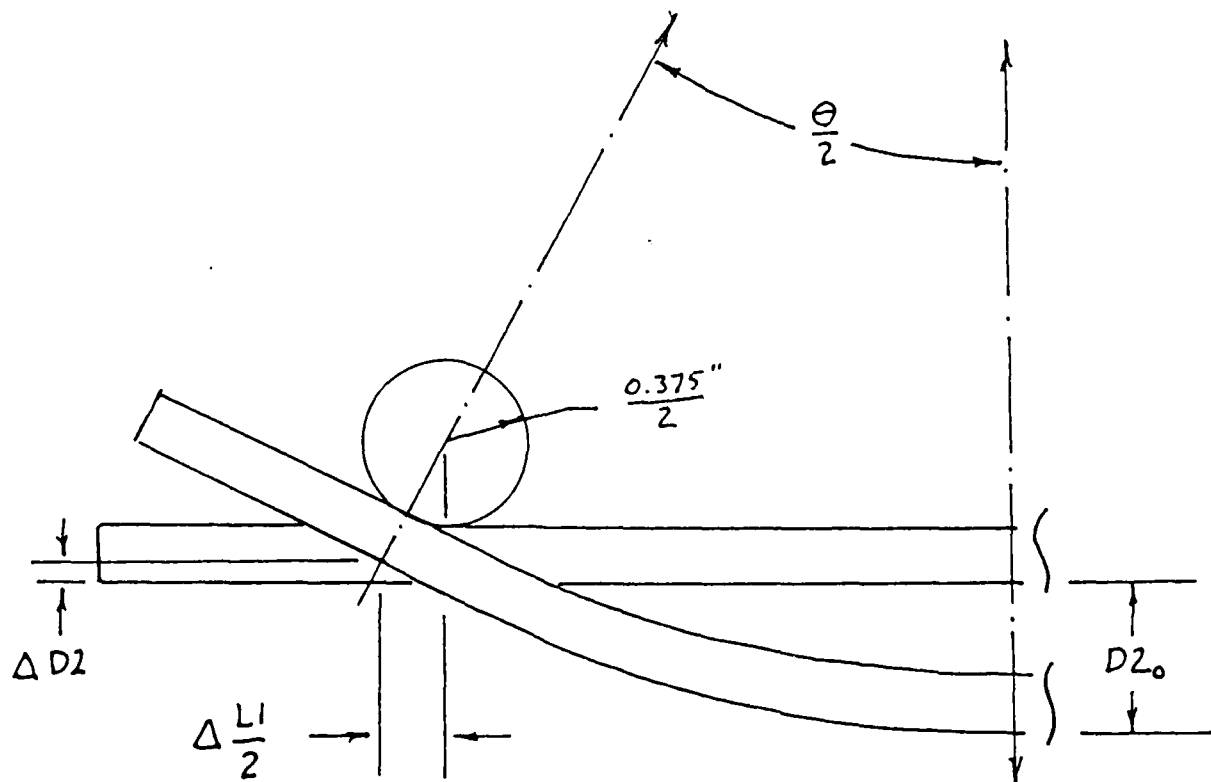


FIGURE A-2: DEFLECTED BEAM WITH ROLLER

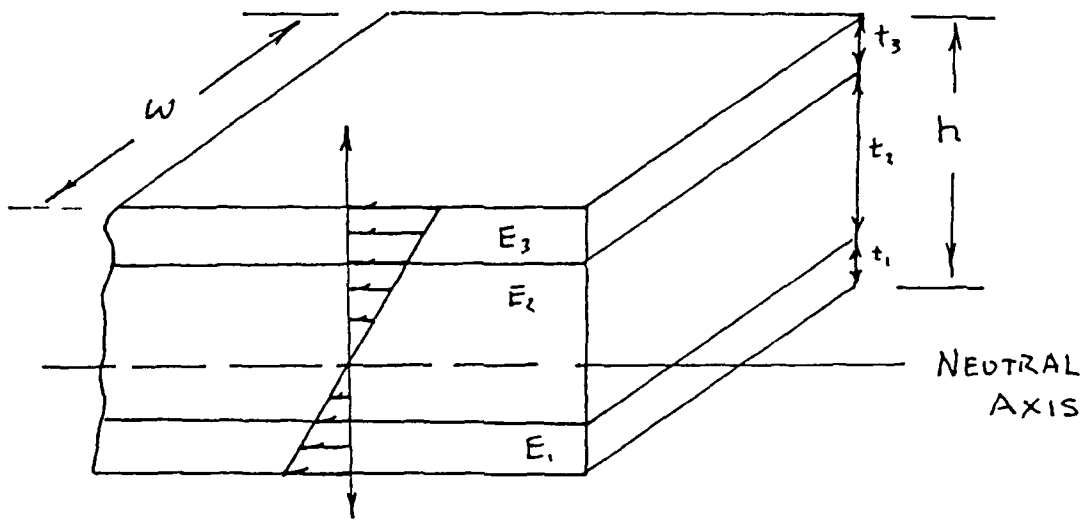


FIGURE B-1: SPECIMEN STRUCTURE

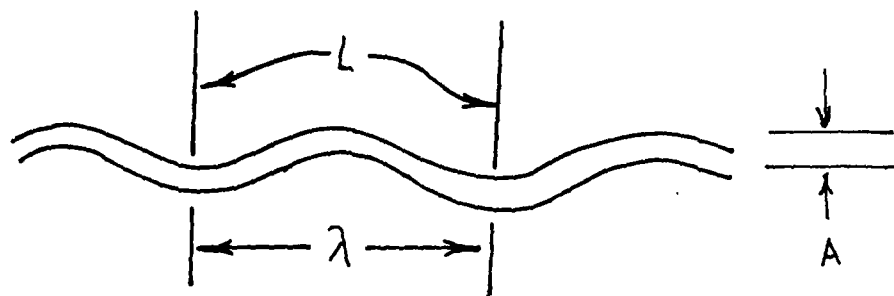


FIGURE E-1: BUCKLED GRAPHITE FIBER

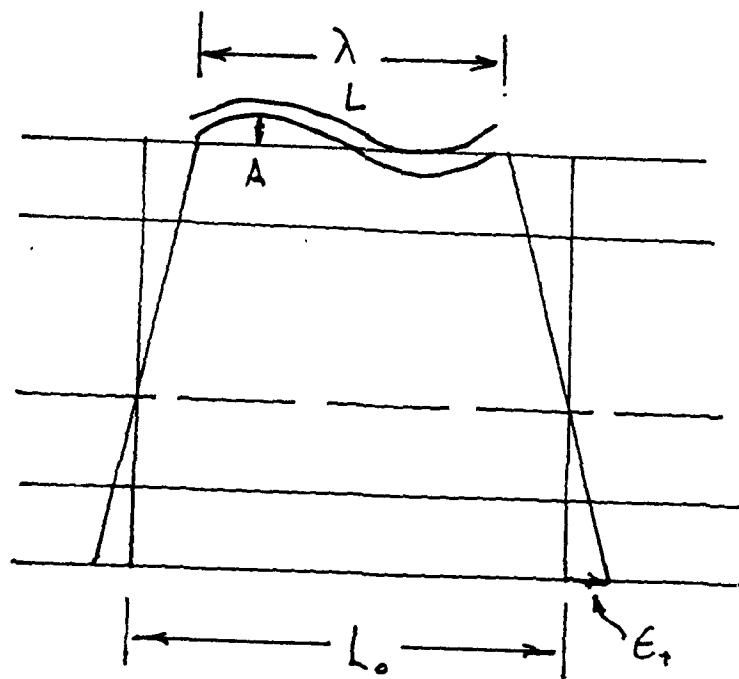


FIGURE F-1: SPECIMEN GEOMETRY UNDER STRAIN

### Appendix A: Radius of Curvature

The specimen geometry is shown in Figure A-1. From the expression for the sector of a circle, we have (A-1) which relates the distances in Figure A-1 to give the radius of curvature  $R$ , of the specimen in terms of the measured deflection,  $D_2$ , of the bottom of the specimen.

$$R = (L_1^2 / 8D_2 + D_2 / 2) \quad (A-1)$$

$$\Theta = (2 \sin^{-1}[L_2 / 2R]) \quad (A-2)$$

To minimize local point loads and to reduce to zero any frictional forces on the specimen due to the holding fixture, the point contacts illustrated in Fig.A1 are, in the actual mount, replaced with rollers as shown in Fig.A-2. The distances,  $D_2$  and  $L_2$  in Eq.A1 must be corrected as follows.

$$D_2 = (D_{2\theta}) + ([h + 0.375/2][1 - \cos(\Theta/2)]) \quad (A-3)$$

$$L_2 = (L_{2\theta}) + ([h + 0.375/2][\sin(\Theta/2)]) \quad (A-4)$$

In the actual geometry used in the experiment, these corrections turned out to be small. Other possible corrections were not made. For example the compressibility of the specimens in the vertical or  $z$  direction was not included in the calculations. It was decided to make a basic check on the determination of radius of curvature by actually building stiff forms with known radii of curvature and bending the specimens over them in order to actually confirm the expressions in this appendix. The expressions proved accurate to the degree needed in the interpretations of the present data.

### Appendix B: Neutral Axis Calculation

The neutral axis of the specimens which were used in this work was calculated for the geometry and parameters as shown in Figure B-1. Assuming that the specimen is deflected such that at a point,  $x$ , along the specimen it has a radius of curvature  $R$ , then the strain at any distance,  $z$ , from the neutral axis is given by (B-1).

$$\epsilon = z/R \quad (B-1)$$

The corresponding strains are indicated in Figure B-1. Using the fact that the integral sum of horizontal forces must be zero, we have (B-2)

$$\int_{-(n+t_1)}^{t_2-n} E_1(z/R) w dz + \int_{-n}^{t_1-t_3-n} E_2(z/R) w dz + \int_{t_1-n}^{t_2-t_3} E_3(z/R) w dz = 0 \quad (B-2)$$

When (B-2) is solved for the distance,  $n$ , which is the distance from the neutral axis to the top of the bottom layer, we get (B-3) which expresses  $n$  in terms of specimen moduli and distances, as shown in Figure B-1.

$$n = \frac{[E_1 t_1^2 + E_3 t_3^2 + 2E_3 t_1 t_3 - E_1 t_1^2]}{2 [E_1 t_1 + E_2 t_2 + E_3 t_3]} \quad (B-3)$$

34

### Appendix C: Strains and Strain Ratios in the Absence of Microbuckling

Again referring to Figure B-1, the strain on the top, compressive surface is given in (C-1)

$$\epsilon_c = z/R \Big|_{z=t_1+t_3-n} = (t_2 + t_3 - n)/R \quad (C-1)$$

The strain on the bottom, tensile surface is given in (C-2)

$$\epsilon_t = z/R \Big|_{z=n+t_1} = (t_1 + n)/R \quad (C-2)$$

The strain ratio, F, is the ratio,  $\epsilon_c/\epsilon_t$ .

$$F = \epsilon_c/\epsilon_t = (t_2 + t_3 - n)/(t_1 + n) \quad (C-3)$$

### Appendix D: Resistance Changes in a Strained Conductor

$R_i = L_o/A_o$ , assuming that  $\rho$  is constant during strain.  $\rho$  is the electrical resistivity of the material,  $L_o$  is the original length, and  $A_o$  is the original area. The new length is  $L$ , the new area is  $A$ , and the change in length is  $\Delta L$ .

The longitudinal strain,  $\epsilon = \Delta L/L_o$

The transverse strain,  $\epsilon_T = \Delta r/r_o = P(\Delta L/L_o) = P\epsilon$  where  $P$  is Poisson's ratio.

$$A = (2\pi r_o)\Delta r = (2\pi r_o P)(r_o P\epsilon) = 2\pi r_o^2 P\epsilon$$

$$\text{Therefore, } R = \rho[(L_o + \Delta L)/(A_o - \Delta A)]$$

$$= \rho[(L_o + \epsilon L_o)/(A_o - 2\pi(r_o)^2 P\epsilon)]$$

$$= \rho[(L_o(1+\epsilon))/(A_o(1-2P\epsilon))]$$

$$\text{or, } R = R_i[(1+\epsilon)/(1-2P\epsilon)]$$

## Appendix E: Length of Microbuckled Graphite

The graphite fibers in the compressed upper layer of the specimen will not only shorten along their length, as is expected in compression, but will also microbuckle as shown in Figure E-1. In order to determine the amplitude of the waveform in terms of the lengths in the figure, the following mathematical steps are required. The waveform is taken to be a sine wave.

$$z = A \sin(2\pi x/\lambda) \quad (E-1)$$

The derivative of z is given in (E-2)

$$dz/dx = A(2\pi/\lambda) \cos(2\pi x/\lambda) \quad (E-2)$$

The differential of length, dL, is given in (E-3)

$$dL = (dx^2 + dz^2)^{1/2} = (dx^2 + ((dz/dx)dx)^2)^{1/2} = dx(1+(dz/dx)^2)^{1/2} \quad (E-3)$$

To get the length, L/4, we integrate dL over x from 0 to  $\lambda/4$

$$L/4 = \int_0^{\lambda/4} [1+(2\pi A/\lambda)^2 (\cos^2(2\pi x/\lambda))] dx \quad (E-4)$$

In order to put this expression into a standard form, we make the following substitutions

$$a = 2\pi A/\lambda \quad (E-5)$$

$$(\sin(\alpha))^2 = a^2/(1+a^2) \quad (E-6)$$

$$\theta = 2\pi x/\lambda \quad (E-7)$$

With these substitutions, the final expression for L/ is given in (E-8)

$$L/\lambda = 2/\pi (1+a^2)^{1/2} \int_0^{\pi/2} (1-\sin^2(\alpha)\sin^2(\theta))^{1/2} d\theta \quad (E-8)$$

The expression in (E-8) is that for an elliptic integral of the second kind. It cannot be evaluated in closed form but was evaluated by numerical integration for the values needed in the interpretation of this experiment. The results are given in Table E-1.

TABLE E-1

 $L' \lambda$ 

A/L

38

1.00000	0.000000
1.00000	0.000278
1.00000	0.000417
1.00000	0.000556
1.00001	0.000694
1.00001	0.000833
1.00001	0.000972
1.00001	0.001111
1.00001	0.001250
1.00002	0.001389
1.00002	0.001528
1.00003	0.001667
1.00004	0.001806
1.00004	0.001945
1.00004	0.002083
1.00005	0.002222
1.00006	0.002361
1.00006	0.002500
1.00007	0.002639
1.00008	0.002778
1.00008	0.002917
1.00009	0.003056
1.00010	0.003195
1.00011	0.003334
1.00012	0.003473
1.00013	0.003612
1.00014	0.003751
1.00015	0.003890
1.00016	0.004029
1.00017	0.004168
1.00018	0.004307
1.00020	0.004446
1.00021	0.004585
1.00022	0.004724
1.00023	0.004863
1.00025	0.005002
1.00026	0.005141
1.00027	0.005280
1.00029	0.005419
1.00030	0.005558
1.00032	0.005697
1.00034	0.005836
1.00035	0.005975
1.00037	0.006114
1.00039	0.006253
1.00040	0.006392
1.00042	0.006531

One typical specimen is illustrated in Figure B-1. The average thicknesses are  $t_1 = 15.8 \times 10^{-3}$  in.,  $t_2 = 42.3 \times 10^{-3}$  in., and  $t_3 = 15.2 \times 10^{-3}$  in. We measured the modulus of our graphite composite in tension and found it to be  $E = 11.63 \times 10^6$  psi. This compares closely with the published figure of  $12 \times 10^6$  psi. We measure the modulus for our bidirectional glass composite,  $E_g$ , and found it to be  $2.62 \times 10^6$  psi.

We now assume that the modulus of our graphite in compression is given by the product of the published ratio of the moduli and our measured modulus in tension. Therefore,  $E_3$ , our assumed modulus in compression is  $8.72 \times 10^6$  psi.

The neutral axis and the predicted ratio of strain in compression to strain in tension is calculated as indicated in Appendices B and C. The location of the neutral axis is indicated in Figure B-1. For the specimen under study, the predicted ratio of strain in compression to strain in tension is 1.196.

For this specimen, we found that the ratio of the strain gauge reading in compression to that in tension was 1.01. We conclude that the graphite was compressed only slightly more than it was tensioned in spite of the fact that the neutral axis is much closer to the graphite in tension. The obvious way to account for the additional compression is with the microbuckling assumption. This is illustrated in Figure F-1.  $L_0$  is the unstrained length of surface which is ultimately compressed to one observed wavelength,  $\lambda$ , of microbuckling. We shall assume  $\epsilon_T$  to be the strain on the surface in tension. By basic theory, we get (F-1)

$$\frac{\lambda}{L_0} = (1 - 1.196 \epsilon_T) \quad (F-1)$$

From our own compressive strain gauge reading, we get (F-2)

$$\frac{L}{L_0} = (1 - 1.01 \epsilon_T) \quad (F-2)$$

Uniting Eq. F-1 and Eq. F-2, we get

$$\frac{L}{\lambda} = (1 - 1.01 \epsilon_T) / (1 - 1.196 \epsilon_T) = (1 + 0.186 \epsilon_T) \quad (F-3)$$

In Table E-1 in Appendix E, we tabulate the ratio of  $A/L$ , the amplitude to the length, against  $L/\lambda$ , the ratio of

curve length to wavelength.

In this particular specimen, when the machine deflection was 0.090 inches, we had a measured tensile strain of  $1837 \times 10^{-6}$ . The ratio of  $L/\lambda$  was then given in (F-4)

$$\frac{L}{\lambda} = [1 + (0.186)(1837 \times 10^{-6})] = 1 + 341 \times 10^{-6} \quad (\text{F-4})$$

Table E-1 give the corresponding value of  $A/L$  to be as follows

$$A/L = 0.006 \quad (\text{F-5})$$

The conclusion is that for  $L = 0.050$ , the amplitude of the microbuckling,  $A$ , is given in (F-6)

$$A = (0.006)(0.050) = 300 \times 10^{-6} \text{ inches} \quad (\text{F-6})$$

This amplitude results in the following additional strains in the compressed surface. If we have a sine wave with amplitude  $A$  and wavelength  $\lambda$ , its expression is given in (F-7)

$$z = A \sin(2\pi x/\lambda) \quad (\text{F-7})$$

The curvature of the sine wave is usefully approximated by the second derivative

$$d^2 z/dx^2 = -A(2\pi/\lambda)^2 \sin(2\pi x/\lambda) \quad (\text{F-8})$$

The strain in a curved surface is known to be the product of the distance from the neutral axis to the point at which the strain is experienced. We now assume that the neutral axis of the graphite is its center. That is, we assume microbuckling to the microbuckling. The peak strain is given in (F-9)

$$\epsilon_{\text{peak}} = (t_3)/2 [(A/L)L](2\pi/\lambda)^2 \quad (\text{F-9})$$

We evaluate  $\epsilon_{\text{peak}}$  to be 0.036. That is, an additional alternating strain with a peak value of 0.036 is added to the compressive strain already present. This is easily enough to cause failure and we attribute specimen failure to it.